AAV1/2-mediated *CNS* Gene Delivery of Dominant-negative CCL2 Mutant Suppresses Gliosis, β-amyloidosis, and Learning Impairment of APP/PS1 Mice

Tomomi Kiyota[1,2], Masaru Yamamoto[1,2], Bryce Schroder[1,2], Michael T Jacobsen[1,2], Russell J Swan[1,2], Mary P Lambert[3], William L Klein[3], Howard E Gendelman[1,2,4], Richard M Ransohoff[5] and Tsuneya Ikezu[1,2,6]

[1]Center for Neurovirology and Neurodegenerative Disorders, University of Nebraska Medical Center, Omaha, Nebraska, USA; [2]Department of Pharmacology and Experimental Neuroscience, University of Nebraska Medical Center, Omaha, Nebraska, USA; [3]Department of Neurobiology and Physiology, Northwestern University, Evanston, Illinois, USA; [4]Department of Internal Medicine, University of Nebraska Medical Center, Omaha, Nebraska, USA; [5]Department of Neurosciences, Lerner Research Institute, Cleveland Clinic Foundation, Cleveland, Ohio, USA; [6]Department of Pathology and Microbiology, University of Nebraska Medical Center, Omaha, Nebraska, USA

Accumulation of aggregated amyloid-β (Aβ) peptide was studied as an initial step for Alzheimer's disease (AD) pathogenesis. Following amyloid plaque formation, reactive microglia and astrocytes accumulate around plaques and cause neuroinflammation. Here brain chemokines play a major role for the glial accumulation. We have previously shown that transgenic overexpression of chemokine CCL2 in the brain results in increased microglial accumulation and diffuse amyloid plaque deposition in a transgenic mouse model of AD expressing Swedish amyloid precursor protein (APP) mutant. Here, we report that adeno-associated virus (AAV) serotype 1 and 2 hybrid efficiently deliver *7ND* gene, a dominant-negative CCL2 mutant, in a dose–response manner and express >1,000-fold higher recombinant CCL2 than basal levels after a single administration. AAV1/2 hybrid virus principally infected neurons without neuroinflammation with sustained expression for 6-months. 7ND expressed in APP/presenilin-1 (APP/PS1) bigenic mice reduced astro/microgliosis, β-amyloidosis, including suppression of both fibrillar and oligomer Aβ accumulation, and improved spatial learning. Our data support the idea that the AAV1/2 system is a useful tool for *CNS* gene delivery, and suppression of CCL2 may be a therapeutic target for the amelioration of AD-related neuroinflammation.

Received 2 September 2008; accepted 11 February 2009; published online 10 March 2009. doi:10.1038/mt.2009.44

INTRODUCTION

The onset of Alzheimer's disease (AD) is significantly associated with astro- and microgliosis associated inflammation.[1] Generally, neuroinflammation elicits neuroprotection in response to changes in the brain's environment and speeds clearance of damaged tissue or harmful substances. However, under the progressive neurodegeneration, such as AD, Parkinson's disease and multiple sclerosis, neuroinflammation can also harm neuronal cells through production of cytotoxic molecules (such as proinflammatory cytokines, complements, excitotoxins, and reactive oxygen species) (for recent review, see ref. 2). β-amyloidosis in AD is modulated by a large number of proinflammatory cytokines, and chemokines, such as interferon-γ, tumor necrosis factor-α, interleukin-1α/β, interleukin-6, interleukin-8, transforming growth factor-β, CD40L, and CCL2 (formally monocyte chemotactic protein-1, MCP-1).[2–4] For instance, interferon-γ, in conjunction with tumor necrosis factor-α enhances amyloid precursor protein (APP) mRNA transcription and amyloid-β (Aβ) production[5,6] and suppresses Aβ degradation.[7] APP mice deficient in CD40L or TNFR1 show reduced Aβ deposition, astro/microgliosis,[8,9] suggesting that elevated expression of proinflammatory cytokines are significantly associated with Aβ production in the brain.

CCL2 is a member of the β chemokine subfamily and a signaling ligand as a homodimer for its cognate G-protein coupled receptor CCR2 A/B.[10] Activated astrocytes and cells of monocytic origin express CCL2 in the brain.[11,12] CCL2 is as a mediator of glial activation upon Aβ stimulation and has been detected in senile plaques and reactive microglia[13,14] as well as microvessels[15] in AD brains. To understand the role of CCL2 in AD pathogenesis, we developed a novel animal model (APP/CCL2)[16] by crossing an established Aβ deposition mouse model (Tg2576), which mimics microglial-induced brain inflammation,[17,18] with a CCL2 overexpressing mouse (JE-95).[19] We previously showed that CCL2 overexpression within the CNS induced microglial activation and increased diffuse plaque formation. APP/CCL2 mice show early onset of spatial learning impairment, synaptic dysfunction, and enhanced Aβ oligomer formation (manuscript submitted). Therefore, the proinflammatory cytokines and chemokines such as CCL2 may be potentially therapeutic targets of AD, and our cumulative hypothesis is that increased intrathecal CCL2 is deleterious to APP transgenic mice and that

Correspondence: *Tsuneya Ikezu, 985880 Nebraska Medical Center, Omaha, Nebraska 68198-5880, USA. E-mail: tikezu@unmc.edu*

a specific and targeted reduction in intrathecal CNS signaling of CCL2 is beneficial.

To address this hypothesis, we developed a viral gene delivery system to overexpress a dominant-negative CCL2 mutant, which is an N-terminal deletion of CCL2 (7ND) and functions as a CCL2 inhibitor to form a heterodimer with endogenous CCL2 *in vitro* and *in vivo*.[20,21] We employed an adeno-associated virus (AAV)-mediated gene delivery approach for introducing 7ND. This method has several advantages over other virus-based brain gene delivery systems: (i) minimal immune response compared to adenovirus or herpes simplex virus infections;[22] (ii) capable of infecting both dividing and nondividing cells without spontaneous tumorigenesis as often found with retroviral vectors; and (iii) persistent transgene expression for >1 year after administration in adult retina[23,24] and brain.[25] The AAV1-derived system shows global gene expression in the brain compared to that of AAV2 expressing predominantly in dentate gyrus after intraventricular injection of neonate animal brains.[26] We have employed the AAV1/2 hybrid virus system to deliver 7ND to APP/presenilin-1 (APP/PS1) bigenic mice in this study. Our approach resulted in robust chronic gene expression in CNS, reduced microglial activation, and lower Aβ deposition.

RESULTS

AAV-mediated expression of dominant-negative CCL2 (7ND) in the brain

To achieve long-term expression of the dominant-negative CCL2 mutant (7ND) in the brain, we developed an AAV1/2-mediated somatic gene transfer system. AAV-7ND virus particles that express murine 7ND or AAV-green fluorescent protein (GFP) as a control were intracranially injected into the frontal cortex or hippocampus of non-Tg mice, and the total amounts of CCL2 and 7ND were then measured by ELISA.

AAV-7ND injection produces strong 7ND protein expression 2 months after injection in a dose-dependent manner [319–104,551 pg/mg of CCL2/7ND and 3×10^8 to 2×10^{10} viral particles (VP)], whereas injection of control AAV-GFP showed no increase (37–48 pg/mg of CCL2 at same doses) (**Figure 1a,b**), suggesting that most of the 7ND or CCL2 in AAV-7ND injected brain was 7ND recombinant protein. We also examined the time course of 7ND expression from 1 to 24 weeks (**Figure 1c**). 7ND was expressed at 14,000, 17,300, 70,000, 161,000, and 97,000 pg/mg at 1, 2, 4, 12, and 24 weeks, respectively, after the injection of 2×10^{10} AAV-7ND VP, whereas control AAV-GFP injected mice expressed 42–394 pg/mg of CCL2 over the same time period, demonstrating long-term expression of recombinant protein. According to the *in vitro* study, a tenfold excess amount of 7ND significantly blocks the bioactivity of CCL2.[27] Thus, the amount of 7ND recombinant protein is sufficient to inhibit CCL2 protein expressed in the brain of APP/PS1 mice (2,771 ± 334.3 and 4,026 ± 781.7 pg/mg brain at 7 and 12 months of age, respectively), a cross-breeding of Tg2576 and M146L presenilin-1 familial AD mutant transgenic line.[17,28] Interestingly, there was no increase in circulating CCL2 levels in plasma between AAV-7ND and AAV-GFP groups 3 months after intracranial injection ($P = 0.7947$, **Figure 1d**). This suggests that the tightly sealed blood brain barrier prevents 7ND leakage from the brain parenchyma,

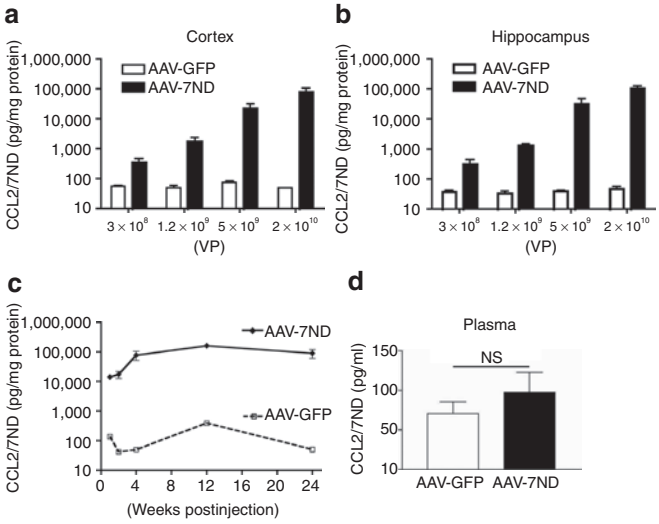

Figure 1 AAV-mediated somatic gene transfer of 7ND and GFP. (**a**,**b**) Non-tg mice at 3 months of age were stereotactically injected with AAV-7ND or AAV-GFP into cortex (**a**) or hippocampus (**b**) at different doses [3×10^8, 1.2×10^9, 5×10^9 and 2×10^{10} viral particles (VP)/brain], and sacrificed 1 month postinjection. The amount of 7ND/CCL2 in brain protein extracts was quantified by CCL2 ELISA. (**c**) Sustained expression of 7ND/CCL2 was observed after hippocampal injection of AAV-7ND or AAV-GFP (2×10^{10} VP/2 µl/site). (**d**) Plasma CCL2 levels at 3 months after intracranial injection of AAV-7ND or GFP. Error bars represent mean + SEM ($n = 3$). AAV, adeno-associated virus; GFP, green fluorescent protein; NS, not significant.

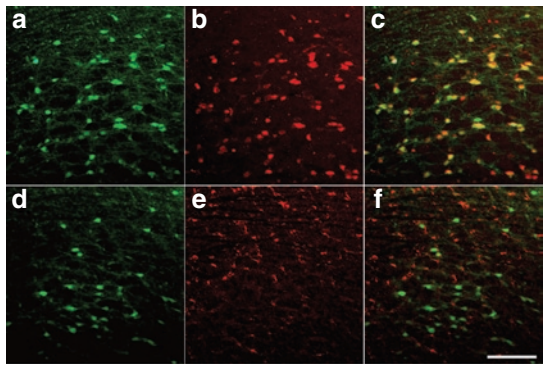

Figure 2 GFP expression of AAV1/2-infected cells in mouse brain. Immunofluorescence of cortical brain sections from mice sacrificed 2 months after hippocampal injection of 2×10^{10} VP AAV1/2-GFP. (**a–c**) GFP (autofluorescence from infected cells) (**a**), anti-NeuN (a neuronal marker) (**b**), and merged image (**c**). (**d–f**) GFP (infected cells) (**d**), anti-GFAP (an astrocytic marker) (**e**), and merged image (**f**). Original magnification: ×100 (×10 objectives). Bar = 200 µm. AAV, adeno-associated virus; GFP, green fluorescent protein.

and blood brain barrier disruption may be necessary for the recruitment of peripheral $CCR2^+$ positive monocytes into brain parenchyma. The AAV-GFP-injected brain was subjected to immunofluorescence to identify AAV-infected cells in the brain (**Figure 2a–f**). The GFP-positive cells are mainly NeuN-positive, a marker of neurons (**Figure 2a–c**), and rarely GFAP-positive, a marker of astrocytes (**Figure 2d–f**). The GFP-positive cells are not associated with gliosis (**Figure 2d–f**), suggesting the lack of neuroinflammation at 2 months after the gene delivery in this system.

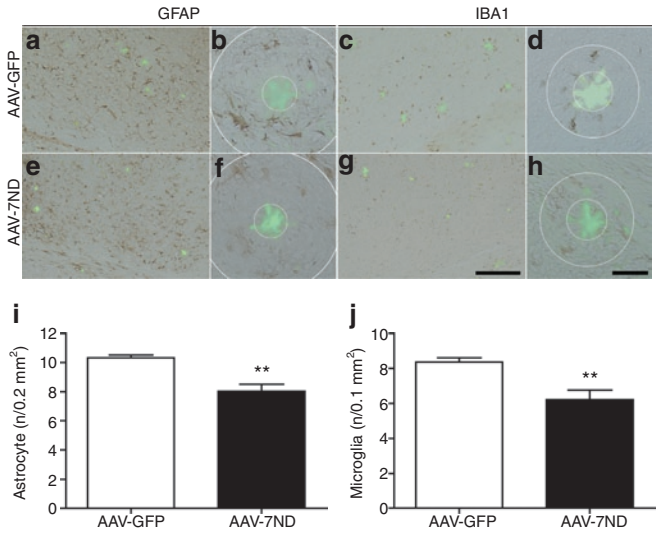

Figure 3 Gene delivery of 7ND suppresses glial accumulation in APP/PS1 mice. (**a–h**) APP/PS1 mice injected with AAV-GFP (**a–d**) or AAV-7ND (**e–h**) (2×10^{10} VP/2 µl/site) into hippocampus at 3 months of age were sacrificed at 8 months of age. The hippocampal frozen sections were immunostained for GFAP (**a,b,e,f**) or IBA1 (**c,d,g,h**), and counterstained by thioflavin-S for compact plaque. Bar = 200 µm in **a,c,e,g**; Bar = 40 µm in **b,d,f,h**. (**i,j**) Quantification of GFAP (**i**) or IBA1 (**j**)-positive cells surrounding thioflavin-S-positive amyloid plaques (cells found in annulus, **b,d,f,h**); radii of outer concentric circles in GFAP (**i**)-positive cells were 60 µm greater than the inner circles that surround amyloid-β (**b,f**), and 30 µm greater in IBA1 (**j**)-positive cells (**d,h**). Error bars for **i** and **j** represent mean + SEM ($n = 5$ per group, 10 sections per brain). ** denotes $P < 0.01$ as determined by Student's *t*-test. AAV, adeno-associated virus; APP, amyloid precursor protein; APP/PS1, APP/presenilin-1; GFP, green fluorescent protein.

Table 1 Amounts of Aβ42 in hippocampus

Fractions	Age (months)	Aβ42 amount (ng)		*t*-test
		AAV-GFP	AAV-7ND	*P* values
SDS-soluble	8	18.62 ± 2.802	13.58 ± 1.572	$P = 0.1728$
SDS-insoluble	8	142.5 ± 87.60	87.60 ± 23.61	$P = 0.2344$
SDS-soluble	12	18.30 ± 3.397	5.545 ± 2.329	$P = 0.0363$*
SDS-insoluble	12	10,437 ± 3,279	7,473 ± 899.6	$P = 0.4327$

Abbreviations: AAV, adeno-associated virus; Aβ, amyloid-β; GFP, green fluorescent protein; SDS, sodium dodecyl sulfate.
Data are group means ± SEM. The *t*-test was used for statistical analysis.
*$P < 0.05$.

Dominant-negative CCL2 suppresses gliosis and β-amyloidosis in aged APP/PS1 bigenic mice

APP/PS1 mice show accelerated Aβ deposition and memory impairment when compared to Tg2576.[29] Based on our previous results, we hypothesized that treatment of APP/PS1 mice with AAV-7ND can correct Aβ-related pathology. AAV-7ND and control AAV-GFP viruses were stereotaxically injected into bilateral hippocampal regions of APP/PS1 mice at 3 months of age, with neuropathological analysis performed at 8 months. Chronic expression of 7ND in APP/PS1 brain reduced astro/microglial accumulation around the β-sheet structure-specific thioflavin-S-positive plaques, which labels β-sheet forming compact plaques, compared to control GFP-expressing APP/PS1 brain (78.1 and 74.2% of AAV-GFP injected APP/PS1 mouse group for

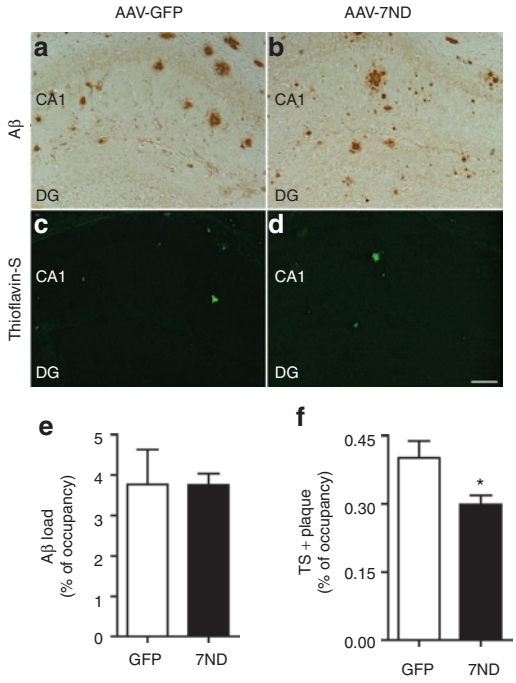

Figure 4 Reduced fibrillar amyloid-β (Aβ) deposition in the hippocampal region of APP/PS1 mice. (**a–d**) Hippocampal frozen sections of APP/PS1 mouse brain injected with AAV-GFP (**a,c**) or AAV-7ND injected (**b,d**) were immunostained with anti-Aβ (**a,b**) polyclonal antibodies, and counterstained by Thioflavin-S (TS) for compact plaque (**c,d**). Bar = 200 µm. (**e,f**) Total Aβ load (**e**) and TS-positive area (**f**) in hippocampal region were quantified in AAV-GFP (GFP) or AAV-7ND (7ND) injected APP/PS1 mice ($n = 5$ per group, 10 sections per brain). * denotes $P < 0.05$ as determined by Student's *t*-test. AAV, adeno-associated virus; APP, amyloid precursor protein; APP/PS1, APP/presenilin-1; GFP, green fluorescent protein.

astrocytes and microglia, respectively, Figure 3a–j), demonstrating suppression of astro/microgliosis.

Since accumulation of astrocytes and microglia are correlated with amyloid plaque deposition,[6,9,30] we examined if 7ND expression suppresses β-amyloidosis in APP/PS1 mice. First, we evaluated the Aβ42 levels by Aβ42 ELISA as described.[16] Both sodium dodecyl sulfate (SDS)-soluble and SDS-insoluble Aβ42 peptides were unchanged by 7ND expression at 8 months of age (Table 1). Next, we examined the area of Aβ loads in the hippocampus of AAV-injected APP/PS1 mice. β-amyloidosis is the process of Aβ aggregation from forming oligomers (detected by specific antioligomer antibodies) to diffuse plaques (detected by pan anti-Aβ antibody), and eventually compact plaques (thioflavin-S-positive plaques). Although total Aβ load, as determined by anti-Aβ staining, was unchanged by 7ND expression (99.7% of AAV-GFP-injected APP/PS1 mouse group, Figure 4, upper panel, 3.77 ± 0.86% in GFP and 3.75 ± 0.27% in 7ND), 7ND significantly reduced thioflavin-S-positive fibrillar Aβ deposition in the hippocampal region (74.4% of AAV-GFP-injected APP/PS1 mouse group, Figure 4, lower panel, 0.40 ± 0.04% in GFP and 0.30 ± 0.02% in 7ND). Accumulating evidences suggest that Aβ oligomer is the Aβ aggregate species that mediates memory impairment and neurophysiological dysfunction in transgenic animal models and AD specimens,[31,32] and it has been the focus of the characterization of β-amyloidosis. Quantification of Aβ oligomers by immunohistochemistry using NU-1 and NU-2, antioligomeric Aβ antibodies, shows significant reduction

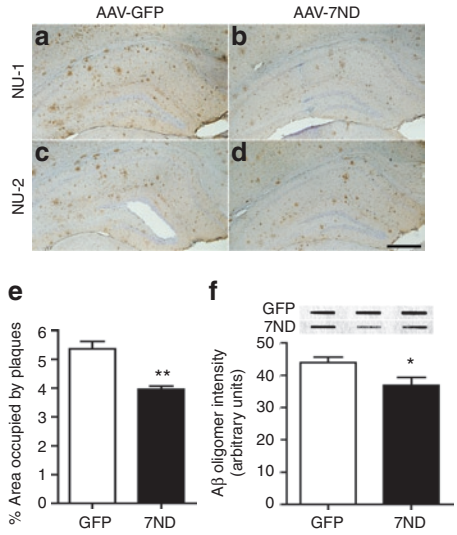

Figure 5 Reduced amyloid-β (Aβ) oligomer deposition in the hippocampal region of APP/PS1 mice. (**a–d**) Frozen sections of AAV-GFP (**a,c**) or AAV-7ND injected APP/PS1 mice (**b,d**) as described in the previous study were immunostained with NU-1 (**a–b**) and NU-2 (**c,d**) monoclonal antibodies specific to Aβ oligomer. Bar = 200 µm. (**e**) Quantification of Aβ oligomers stained with NU-1 in hippocampal region after AAV-GFP (GFP) or AAV-7ND (7ND) injection (n = 5 per group, 10 sections per brain). (**f**) Dot-blot studies of Aβ oligomers using sodium dodecyl sulfate-soluble fraction of AAV-GFP (GFP) or AAV-7ND (7ND)-injected APP/PS1 mice (n = 4 per group, representative images shown). Band luminescent intensities detected with NU-1 were quantified by Typhoon Phosphoimager. * and ** denote $P < 0.05$ and 0.01, respectively, as determined by Student's t-test. AAV, adeno-associated virus; APP, amyloid precursor protein; APP/PS1, APP/presenilin-1; GFP, green fluorescent protein.

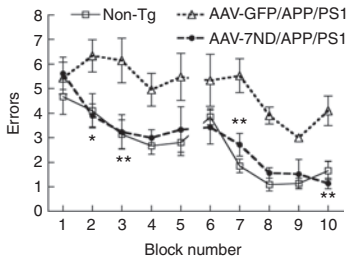

Figure 6 Gene delivery of 7ND improves memory function of APP/PS1 mice. APP/PS1 mice received bilateral hippocampal injection of AAV-7ND or AAV-GFP (2×10^{10} VP/2 µl/site) at 10 months of age, and tested by 2-day radial arm water maze task at 12 months of age (n = 8 per group). Non-tg group (n = 8) serves as positive control of the spatial learning task. * or ** denotes $P < 0.05$ or 0.01 of AAV-7ND versus AAV-GFP group as determined by two-way repeated measures analysis of variance and Bonferroni post-test. AAV, adeno-associated virus; APP, amyloid precursor protein; APP/PS1, APP/presenilin-1; GFP, green fluorescent protein.

of Aβ oligomer load in AAV-7ND injected group as compared to AAV-GFP injected group at 8 months of age (73.8% of AAV-GFP-injected APP/PS1 mouse group, **Figure 5a–e**, 5.37 ± 0.26% in GFP and 3.96 ± 0.11% in 7ND). Dot-blot with NU-1 performed for ultracentrifuged brain SDS extracts, which do not contain fibrillar Aβ, also shows significant reduction of Aβ oligomer in the AAV-7ND injected group (**Figure 5f**). These data suggest that chronic inhibition of CCL2 suppresses astroglial/microglial accumulation and β-amyloidosis, specifically fibrillar and oligomer species of Aβ aggregates, in APP/PS1 mice.

Dominant-negative CCL2 suppresses memory impairment in aged APP/PS1 bigenic mice

Finally, we examined if dominant-negative CCL2 improves spatial learning in APP/PS1 mice by 2-day radial arm water maze task (**Figure 6**).[33] Our initial attempt to determine the effect of presymptomatic injection of AAV-7ND on APP/PS1 mice was unsuccessful due to an insignificant difference in spatial learning among non-Tg, APP/PS1 with AAV-7ND, and APP/PS1 with AAV-GFP treatment (data not shown). Thus, we tested the effect of postsymptomatic injection of AAV-7ND in APP/PS1 mice at 10 months of age, with memory function testing at 12 months. The age-matched non-Tg mouse group modeled the representative learning curve. In contrast, the AAV-GFP-injected APP/PS1 mouse group showed significantly higher errors than that of non-Tg group throughout the trials, indicating impaired memory acquisition. However, the AAV-7ND-injected APP/PS1 mouse group showed similar error numbers to the non-Tg group, which is significantly lower than the AAV-GFP group, indicating secured memory acquisition and recall. We also evaluated the Aβ42 levels in the hippocampus of these mouse groups by Aβ42 ELISA (n = 4, **Table 1**). Although SDS-insoluble Aβ42 peptides were unchanged by 7ND expression, SDS-soluble Aβ42 peptides were significantly reduced by 7ND expression at 12 but not 7 months of age (**Table 1**). Taken together, these data suggest that chronic inhibition of CCL2 suppresses astrocyte/microglial responses, Aβ production and aggregation, and improve memory formation in APP/PS1 mice.

DISCUSSION

Our results demonstrate that the AAV1/2 hybrid vector is an efficient *CNS* gene delivery method especially for the expression of a chemokine mutant in the brain due to its high expression level, long-term expression, negligible leak to blood, and minimal inflammatory response after brain parenchymal injection. The AAV1-derived system shows more diffuse gene expression in the brain, whereas the use of the conventional AAV2 vector mainly expresses in the dentate gyrus and with lesser amount of gene expression (data not shown),[26] supporting the use of AAV1/2 hybrid system for more ubiquitous gene delivery in the injected brain region. Using this technology, we have shown that CCL2, which is clinically correlated with AD pathogenesis,[16] can be therapeutically targeted. APP/CCL2 mice show an early onset of spatial learning impairment and Aβ oligomer formation, whereas CCL2 mice show normal learning, suggesting that CCL2 is a cofactor in Aβ-induced memory impairment in APP mice but does not induce memory dysfunction by itself (manuscript submitted).

The mechanism of CCL2 and microglial enhancement of Aβ aggregation remains unknown. Our previous studies ruled out three possibilities: (i) interaction of CCL2 on enhanced Aβ synthesis; (ii) reduced clearance of fibrillar Aβ degradation by bone marrow–derived macrophages; and (iii) reduced clearance of intracranially injected fibrillar Aβ *in vivo*.[16,34] However, we have recently found that monomeric Aβ undergoes rapid oligomer formation in microglia after uptake, which is enhanced by CCL2 and tumor necrosis factor-α (manuscript submitted).

This suggests that microglia generate Aβ oligomer intracellularly, which is secreted and serves as an Aβ oligomer seed for diffuse plaque formation. Thus, blockage of CCL2 by the expression of 7ND may suppress β-amyloidosis via inhibition of microgliosis and direct suppression of intracellular Aβ oligomer formation in microglia.

Disruption of CCR2, a specific CCL2 receptor, inhibits microglial accumulation in APP mice.[35] However, APP/CCR2$^{-/-}$ mice show early onset of amyloid deposition.[35] This could be due to the lack of infiltration by peripheral bone marrow–derived monocytes into the brain.[36] The lack of peripheral monocytes, which play a key role in amyloid clearance, may lead to enhanced Aβ deposition in the brain. Since most AD patients have intact CCL2-CCR2 signaling, suppression of chemokine-mediated mononuclear phagocyte flux via chemokine inhibitors may be of therapeutic interest. Other chemokines, such as interleukin-8, upregulated in MCI and AD patients, also may have similar functions in microgliosis and cognitive dysfunction in AD mouse models. The functions of these other chemokines is a subject of future investigations.

Adenoviral gene delivery of 7ND has been used for the treatment of multiple inflammatory disease animal models *in vivo*, whereas there is only one report of the adenoviral *7ND* gene transfer into animal brain[37] and there were no studies of the AAV-mediated gene transfer of 7ND. We found no difference in the longevity of AAV-7ND injected APP/PS1 mice as compared to AAV-GFP injected group, sociobehavioral activities (diet, sleep, spontaneous activities, motor coordination, aggressiveness, irritation, cleanness, fatigue, etc), or body weight. AAV-mediated gene delivery has been successful in reducing β-amyloidosis in mouse brains by the expression of anti-Aβ single chain variant fragments,[38,39] Aβ degrading enzymes (neprilysin and endothelin converting enzyme),[40,41] recombinant Aβ fusion protein for vaccination,[42–44] and integral membrane protein 2B familial British dementia mutant protein.[45] AAV-mediated Aβ vaccination of APP mice also improved working memory.[42,44] To the best of our knowledge, this is the first time that AAV-mediated gene delivery of a chemokine antagonist into transgenic AD animal models was shown to suppress β-amyloidosis and improve working memory in APP/PS1 mice.

Although nonsteroidal anti-inflammatory drugs have been proposed as prophylactic drugs[46] or drugs capable of ameliorating β-amyloidosis in transgenic amyloid mouse models, none of them were successful in clinical trials except R-flurbiprofen.[47] In addition, nonsteroidal anti-inflammatory drugs have been the subjects of chemical engineering for their γ-secretase modulating activity instead of their original anti-inflammatory activity.[48] Thus, both AAV-mediated anti-inflammatory therapy and γ-secretase modulating drugs may be mutually synergistic for the treatment of β-amyloidosis.

In summary, our study demonstrates the potential of AAV1/2 hybrid-mediated *CNS* gene delivery of chemokine mutants, which may be beneficial to suppress the neuroinflammation and β-amyloidosis, which are detrimental to neuronal function. Further study will determine how a blockade of brain CCL2 could affect clinical AD progression.

MATERIALS AND METHODS

Animals. Tg2576 mice expressing the Swedish mutation of human APP_{695} were obtained from Drs Carlson and Hsiao-Ashe through Mayo Medical Venture.[17] Male Tg2576 were backcrossed at least seven times to the B6/129 strain. PS1 mutant mice (M146L line 6.1) were provided by Dr Duff through University of South Florida, maintained as PS1 transgene homozygote,[28] which have been backcrossed to the B6/129 strain at least five times prior to the crossing. To generate APP/PS1 bigenic mice, Tg2576 mice were crossed with PS1 mice. Age-matched non-Tg mice in B6/129 F1 strain (Jackson laboratory, Bar Harbor, ME) were maintained by intercrossing in the same facility. All animal-use procedures were strictly reviewed by Institutional Animal Care and Use Committee (IACUC) of University of Nebraska Medical Center.

AAV-7ND gene construction. We have constructed an AAV2 vector (pAAV2-MCS-WPRE), which contains cytomegalovirus immediate early enhancer, chicken β-actin promoter with first exon and intron sequences, multiple cloning site (MCS), Woodchuck hepatitis post-transcriptional regulatory element (WPRE), and the bovine growth hormone polyadenylation site, all of which are flanked by AAV2 inverted terminal repeat based on pGFP vector (provided by R. Klein).[49] To construct 7ND, mouse CCL2 was generated by proof-reading PCR amplification of wild type CCL2 (1,516 bp) from mouse genomic DNA and subcloned into the MCS of pUC18 at EcoRI-BamHI sites. After sequencing, the first 7 amino acids after the signal peptide sequence (^{25}PDAVNAP^{31}) were deleted by site-directed mutagenesis. Next, the entire 7ND genomic DNA was subcloned into MCS of pAAV-MCS-WPRE at EcoRI-NheI sites, developing pAAV-MCS-WPRE-7ND. For details of primer sets used for construction of AAV-7ND and generation and purification of AAV1/2 virus, see **Supplementary Materials and Methods**.

Stereotaxic injection. Mice at 3 months of age received i.p. injection of ketamine/xylazine anesthesia (100 mg/kg ketamine and 20 mg/kg xylazine). After mice were immobilized in a stereotaxic apparatus (Stoelting, Wood Dale, IL), a linear skin incision was made over the bregma, and a 1-mm burr hole was drilled in the skull 2.1 mm posterior and 1.8 mm lateral to the bregma on both sides using a hand-held driller. 2 µl of saline containing AAV-GFP or AAV-7ND (2×10^{10} VP) was injected into hippocampus 1.8 mm below the surface of the skull using 10-µl Hamilton syringe.

Immunohistochemistry. Immunohistochemistry was performed as described previously.[6,16] Briefly, mice were euthanized with isoflurane and perfused transcardially with 25 ml of ice-cold PBS. The brains were rapidly removed, immersed in freshly depolymerized 4% paraformaldehyde for 48 hours, and cryoprotected by successive 24-hour immersions in 15% and 30% sucrose in 1× PBS immediately before sectioning. Fixed, cryoprotected brains were frozen and sectioned in the coronal plane using a Cryostat (Leica, Bannockburn, IL), with sections collected serially. Immunohistochemistry was performed using specific antibodies to identify astrocyte (GFAP, rabbit polyclonal, 1:2,000) (DAKO, Glostrup, Denmark), microglia (IBA1, rabbit polyclonal, 1:1,000) (Wako, Richmond, VA), microtubule-associated protein 2 (MAP2) (Chemicon, Temecula, CA), pan-Aβ (1:100) (Zymed, San Francisco, CA), and Aβ oligomer (NU-1 or NU-2 monoclonal, 1 µg/ml) (Northwestern University). Immunodetection was visualized using Envision Plus (DAKO, Carpinteria, CA) with 3,3′-diaminobenzidine (Vector Laboratories, Burlingame, CA). For immunofluorescence, Alexa Fluor 568-conjugated antirabbit IgG (H+L) was used as a secondary antibody. 0.1% Thioflavin S in 50% EtOH was used for counterstaining of compact plaque (Sigma, St Louis, MO). For quantification analysis, the numbers of GFAP-positive astrocytes and IBA1-positive microglia around Aβ plaques in the hippocampus were counted at 100-µm intervals in ten 10-µm coronal sections from each mouse. Three TS-positive plaques were randomly chosen per section, and five brains of mice per group were analyzed (30 plaques per animal). The areas of Aβ loads and TS-positive plaques were analyzed using an image

analysis software (ImageJ, NIH) at 100-μm intervals in ten 10-μm coronal sections from each mouse. Five brains of mice per group were analyzed.

Biochemical and dot-blot analyses. Aβ and CCL2 ELISA were performed as previously described.[6,16,50] Dot-blot analysis for Aβ oligomer was performed as described previously[50] with some modifications. Briefly, mouse brains were homogenized in 2% SDS containing PMSF (0.5 mmol/l), Leupeptin (3 μg/ml), and Aprotinin (5 μg/ml), and centrifuged at 4 °C for 1 hour at 100,000*g*. The supernatant was used for dot-blot. Protein concentration was determined using BCA Protein Assay Kit (Pierce, Rockford, IL). Samples were adjusted with 1× PBS to the same concentration, and applied to a nitrocellulose membrane using Bio-Dot SF Microfiltration Apparatus according to manufacturer's instruction (Bio-Rad, Richmond, CA). After blotting, membrane was incubated in a 5% solution of nonfat dry milk for 1 hour at room temperature. After overnight incubation at 4 °C with primary antibody (clone NU-1; 1 μg/ml), membrane was washed in Tween 20-TBS (TTBS) (0.05% Tween 20, 100 mmol/l Tris, pH 7.5, 150 mmol/l NaCl) for 3 × 10 minutes and incubated at room temperature with the HRP-conjugated antimouse IgG (Jackson ImmunoResearch Laboratories, West Grove, PA) for 1 hour. Membrane was washed in TTBS for 3 × 10 minutes and incubated for 5 minutes with chemiluminescent substrate (ECL Plus; GE Healthcare Bio-Sciences, Piscataway, NJ). Images were taken using an image analyzer (Typhoon; GE Healthcare Bio-Sciences). Band density was measured using ImageQuant software.

Two-day radial arm water maze. The radial arm water maze task was run as described previously with minor modification.[33] Animals were introduced into the perimeter of a circular water-filled tank 110 cm in diameter and 91 cm in height (San Diego Instruments, San Diego, CA) with triangular inserts placed in the tank to produce six swim-paths radiating out from a central area. Spatial cues for mice orientation were present on the walls of the tank. At the end of one arm, a 10 cm circular plexiglass platform was submerged 1 cm deep—hidden from the mice. On day 1, 15 trials (12 trials with visible platform followed by 3 trials with hidden platform) were run in five blocks of 3. A cohort of 4 mice was run sequentially for each block. After each 3-trial block, a second cohort of mice was run permitting an extended rest period before mice were exposed to the second block. The target arm location remained constant for a given mouse throughout the test. Each trial lasts 1 minutes and an error is scored each time the body of the mouse, excluding tail, enters the wrong arm, enters the arm with the platform but does not climb on it, or does not make a choice for 20 seconds. Each trial ends when the mouse climbs onto and remains on the hidden platform for 10 seconds. The mouse is given 20 seconds to rest on the platform between each trial. On day 2, the mice were run in exactly the same manner as day 1, except that the platform was hidden for all trials. Between blocks 4 and 5 on day 1, and blocks 9 and 10 on day 2, additional retention for 30 minutes was given to each mouse to test short-term memory recall. The errors on each block were averaged and used for statistical analysis.

Statistics. All data were normally distributed and presented as mean values ± SEM. In case of single mean comparison, data were analyzed by Student's *t*-test. In case of multiple mean comparisons, the data were analyzed by two-way repeated measures analysis of variance), followed by Bonferroni multiple comparison test using statistics software (Prism 4.0; Graphpad Software, San Diego, CA). *P* values <0.05 were regarded as significant difference.

SUPPLEMENTARY MATERIAL

Materials and Methods.

ACKNOWLEDGMENTS

We thank Drs Hsiao-Ashe for providing Tg2576 mice, Duff for providing M146L PS1 mice, Morgan for radial arm water maze test training and consultation, Klein for pGFP plasmid, and University of Pennsylvania Gene Therapy Program for recombinant AAV1 vectors, and Meg Marquardt for editing of the manuscript. This work is supported by Vada Oldfield Alzheimer Research Foundation (T.I., T.K.), NIH R21 AG032600 (T.I.), NIH R0I AG22547 (W.L.K.), NIH P01 NS043985 (T.I., H.E.G.), and NIH R01 NS32151 (R.M.R.).

REFERENCES

1. Barron, KD (1995). The microglial cell. A historical review. *J Neurol Sci* **134** (suppl.): 57–68.
2. Ikezu, T (2008). Alzheimer's disease. In: Ikezu T, Gendelman HE (eds). *Neuroimmune Pharmacology*. Springer: New York. pp. 343–353.
3. Akiyama, H, Barger, S, Barnum, S, Bradt, B, Bauer, J, Cole, GM *et al.* (2000). Inflammation and Alzheimer's disease. *Neurobiol Aging* **21**: 383–421.
4. McGeer, PL and McGeer, EG (2001). Inflammation, autotoxicity and Alzheimer disease. *Neurobiol Aging* **22**: 799–809.
5. Blasko, I, Marx, F, Steiner, E, Hartmann, T and Grubeck-Loebenstein, B (1999). TNF-α plus IFN-γ induce the production of Alzheimer β-amyloid peptides and decrease the secretion of APPs. *Faseb J* **13**: 63–68.
6. Yamamoto, M, Kiyota, T, Horiba, M, Buescher, JL, Walsh, SM, Gendelman, HE *et al.* (2007). Interferon-γ and tumor necrosis factor-α regulate amyloid-β plaque deposition and β-secretase expression in Swedish mutant app transgenic mice. *Am J Pathol* **170**: 680–692.
7. Yamamoto, M, Kiyota, T, Walsh, SM, Liu, J, Kipnis, J and Ikezu, T (2008). Cytokine-mediated inhibition of fibrillar amyloid-β peptide degradation by human mononuclear phagocytes. *J Immunol* **181**: 3877–3886.
8. Tan, J, Town, T and Mullan, M (2002). CD40-CD40L interaction in Alzheimer's disease. *Curr Opin Pharmacol* **2**: 445–451.
9. He, P, Zhong, Z, Lindholm, K, Berning, L, Lee, W, Lemere, C *et al.* (2007). Deletion of tumor necrosis factor death receptor inhibits amyloid β generation and prevents learning and memory deficits in Alzheimer's mice. *J Cell Biol* **178**: 829–841.
10. Charo, IF, Myers, SJ, Herman, A, Franci, C, Connolly, AJ and Coughlin, SR (1994). Molecular cloning and functional expression of two monocyte chemoattractant protein 1 receptors reveals alternative splicing of the carboxyl-terminal tails. *Proc Natl Acad Sci USA* **91**: 2752–2756.
11. Calvo, CF, Yoshimura, T, Gelman, M and Mallat, M (1996). Production of monocyte chemotactic protein-1 by rat brain macrophages. *Eur J Neurosci* **8**: 1725–1734.
12. Glabinski, AR, Balasingam, V, Tani, M, Kunkel, SL, Strieter, RM, Yong, VW *et al.* (1996). Chemokine monocyte chemoattractant protein-1 is expressed by astrocytes after mechanical injury to the brain. *J Immunol* **156**: 4363–4368.
13. Ishizuka, K, Kimura, T, Igata-yi, R, Katsuragi, S, Takamatsu, J and Miyakawa, T (1997). Identification of monocyte chemoattractant protein-1 in senile plaques and reactive microglia of Alzheimer's disease. *Psychiatry Clin Neurosci* **51**: 135–138.
14. Xia, MQ and Hyman, BT (1999). Chemokines/chemokine receptors in the central nervous system and Alzheimer's disease. *J Neurovirol* **5**: 32–41.
15. Grammas, P and Ovase, R (2001). Inflammatory factors are elevated in brain microvessels in Alzheimer's disease. *Neurobiol Aging* **22**: 837–842.
16. Yamamoto, M, Horiba, M, Buescher, JL, Huang, D, Gendelman, HE, Ransohoff, RM *et al.* (2005). Overexpression of monocyte chemotactic protein-1/CCL2 in β-amyloid precursor protein transgenic mice show accelerated diffuse β-amyloid deposition. *Am J Pathol* **166**: 1475–1485.
17. Hsiao, K, Chapman, P, Nilsen, S, Eckman, C, Harigaya, Y, Younkin, S *et al.* (1996). Correlative memory deficits, Aβ elevation, and amyloid plaques in transgenic mice. *Science* **274**: 99–102.
18. Frautschy, SA, Yang, F, Irrizarry, M, Hyman, B, Saido, TC, Hsaio, K *et al.* (1998). Microglial Response to Amyloid Plaques in APPsw Transgenic Mice. *Am J Pathol* **152**: 307–317.
19. Huang, D, Tani, M, Wang, J, Han, Y, He, TT, Weaver, J *et al.* (2002). Pertussis toxin-induced reversible encephalopathy dependent on monocyte chemoattractant protein-1 overexpression in mice. *J Neurosci* **22**: 10633–10642.
20. Zhang, YJ, Rutledge, BJ and Rollins, BJ (1994). Structure/activity analysis of human monocyte chemoattractant protein-1 (MCP-1) by mutagenesis. Identification of a mutated protein that inhibits MCP-1-mediated monocyte chemotaxis. *J Biol Chem* **269**: 15918–15924.
21. Ikeda, Y, Yonemitsu, Y, Kataoka, C, Kitamoto, S, Yamaoka, T, Nishida, K *et al.* (2002). Anti-monocyte chemoattractant protein-1 gene therapy attenuates pulmonary hypertension in rats. *Am J Physiol Heart Circ Physiol* **283**: H2021–H2028.
22. Xiao, X, Li, J, McCown, TJ and Samulski, RJ (1997). Gene transfer by adeno-associated virus vectors into the central nervous system. *Exp Neurol* **144**: 113–124.
23. Dudus, L, Anand, V, Acland, GM, Chen, SJ, Wilson, JM, Fisher, KJ *et al.* (1999). Persistent transgene product in retina, optic nerve and brain after intraocular injection of rAAV. *Vision Res* **39**: 2545–2553.
24. Guy, J, Qi, X, Muzyczka, N and Hauswirth, WW (1999). Reporter expression persists 1 year after adeno-associated virus-mediated gene transfer to the optic nerve. *Arch Ophthalmol* **117**: 929–937.
25. Peel, AL and Klein, RL (2000). Adeno-associated virus vectors: activity and applications in the CNS. *J Neurosci Methods* **98**: 95–104.
26. Passini, MA, Watson, DJ, Vite, CH, Landsburg, DJ, Feigenbaum, AL and Wolfe, JH (2003). Intraventricular brain injection of adeno-associated virus type 1 (AAV1) in neonatal mice results in complementary patterns of neuronal transduction to AAV2 and total long-term correction of storage lesions in the brains of β-glucuronidase-deficient mice. *J Virol* **77**: 7034–7040.
27. Zhang, Y and Rollins, BJ (1995). A dominant negative inhibitor indicates that monocyte chemoattractant protein 1 functions as a dimer. *Mol Cell Biol* **15**: 4851–4855.
28. Duff, K, Eckman, C, Zehr, C, Yu, X, Prada, CM, Perez-tur, J *et al.* (1996). Increased amyloid-β42(43) in brains of mice expressing mutant presenilin 1. *Nature* **383**: 710–713.

29. Morgan, D, Diamond, DM, Gottschall, PE, Ugen, KE, Dickey, C, Hardy, J *et al.* (2000). Aβ peptide vaccination prevents memory loss in an animal model of Alzheimer's disease. *Nature* **408**: 982–985.
30. Tan, J, Town, T, Crawford, F, Mori, T, DelleDonne, A, Crescentini, R *et al.* (2002). Role of CD40 ligand in amyloidosis in transgenic Alzheimer's mice. *Nat Neurosci* **5**: 1288–1293.
31. Walsh, DM, Klyubin, I, Fadeeva, JV, Cullen, WK, Anwyl, R, Wolfe, MS *et al.* (2002). Naturally secreted oligomers of amyloid β protein potently inhibit hippocampal long-term potentiation *in vivo*. *Nature* **416**: 535–539.
32. Lesné, S, Koh, MT, Kotilinek, L, Kayed, R, Glabe, CG, Yang, A *et al.* (2006). A specific amyloid-β protein assembly in the brain impairs memory. *Nature* **440**: 352–357.
33. Wilcock, DM, Rojiani, A, Rosenthal, A, Subbarao, S, Freeman, MJ, Gordon, MN *et al.* (2004). Passive immunotherapy against Aβ in aged APP-transgenic mice reverses cognitive deficits and depletes parenchymal amyloid deposits in spite of increased vascular amyloid and microhemorrhage. *J Neuroinflammation* **1**: 24.
34. Yamamoto, M, Kiyota, T, Walsh, SM and Ikezu, T (2007). Kinetic analysis of aggregated amyloid-b peptide clearance in adult bone-marrow-derived macrophages from APP and CCL2 transgenic mice. *J Neuroimmune Pharmacol* **2**: 213–221.
35. El Khoury, J, Toft, M, Hickman, SE, Means, TK, Terada, K, Geula, C *et al.* (2007). Ccr2 deficiency impairs microglial accumulation and accelerates progression of Alzheimer-like disease. *Nat Med* **13**: 432–438.
36. Mildner, A, Schmidt, H, Nitsche, M, Merkler, D, Hanisch, UK, Mack, M *et al.* (2007). Microglia in the adult brain arise from Ly-6ChiCCR2^{+} monocytes only under defined host conditions. *Nat Neurosci* **10**: 1544–1553.
37. Kumai, Y, Ooboshi, H, Takada, J, Kamouchi, M, Kitazono, T, Egashira, K *et al.* (2004). Anti-monocyte chemoattractant protein-1 gene therapy protects against focal brain ischemia in hypertensive rats. *J Cereb Blood Flow Metab* **24**: 1359–1368.
38. Fukuchi, K, Tahara, K, Kim, HD, Maxwell, JA, Lewis, TL, Accavitti-Loper, MA *et al.* (2006). Anti-Aβ single-chain antibody delivery via adeno-associated virus for treatment of Alzheimer's disease. *Neurobiol Dis* **23**: 502–511.
39. Wang, YJ, Pollard, A, Zhong, JH, Dong, XY, Wu, XB, Zhou, HD *et al.* (2009). Intramuscular delivery of a single chain antibody gene reduces brain Aβ burden in a mouse model of Alzheimer's disease. *Neurobiol Aging* **30**: 364–376.
40. Iwata, N, Mizukami, H, Shirotani, K, Takaki, Y, Muramatsu, S, Lu, B *et al.* (2004). Presynaptic localization of neprilysin contributes to efficient clearance of amyloid-β peptide in mouse brain. *J Neurosci* **24**: 991–998.
41. Carty, NC, Nash, K, Lee, D, Mercer, M, Gottschall, PE, Meyers, C *et al.* (2008). Adeno-associated viral (AAV) serotype 5 vector mediated gene delivery of endothelin-converting enzyme reduces Aβ deposits in APP + PS1 transgenic mice. *Mol Ther* **16**: 1580–1586.
42. Mouri, A, Noda, Y, Hara, H, Mizoguchi, H, Tabira, T and Nabeshima, T (2007). Oral vaccination with a viral vector containing Aβ cDNA attenuates age-related Aβ accumulation and memory deficits without causing inflammation in a mouse Alzheimer model. *Faseb J* **21**: 2135–2148.
43. Hara, H, Monsonego, A, Yuasa, K, Adachi, K, Xiao, X, Takeda, S *et al.* (2004). Development of a safe oral Aβ vaccine using recombinant adeno-associated virus vector for Alzheimer's disease. *J Alzheimers Dis* **6**: 483–488.
44. Zhang, J, Wu, X, Qin, C, Qi, J, Ma, S, Zhang, H *et al.* (2003). A novel recombinant adeno-associated virus vaccine reduces behavioral impairment and β-amyloid plaques in a mouse model of Alzheimer's disease. *Neurobiol Dis* **14**: 365–379.
45. Kim, J, Miller, VM, Levites, Y, West, KJ, Zwizinski, CW, Moore, BD *et al.* (2008). BRI2 (ITM2b) inhibits Aβ deposition *in vivo*. *J Neurosci* **28**: 6030–6036.
46. Etminan, M, Gill, S and Samii, A (2003). Effect of non-steroidal anti-inflammatory drugs on risk of Alzheimer's disease: systematic review and meta-analysis of observational studies. *BMJ* **327**: 128.
47. Galasko, DR, Graff-Radford, N, May, S, Hendrix, S, Cottrell, BA, Sagi, SA *et al.* (2007). Safety, tolerability, pharmacokinetics, and Aβ levels after short-term administration of R-flurbiprofen in healthy elderly individuals. *Alzheimer Dis Assoc Disord* **21**: 292–299.
48. Kukar, TL, Ladd, TB, Bann, MA, Fraering, PC, Narlawar, R, Maharvi, GM *et al.* (2008). Substrate-targeting γ-secretase modulators. *Nature* **453**: 925–929.
49. Klein, RL, Hamby, ME, Gong, Y, Hirko, AC, Wang, S, Hughes, JA *et al.* (2002). Dose and promoter effects of adeno-associated viral vector for green fluorescent protein expression in the rat brain. *Exp Neurol* **176**: 66–74.
50. Oddo, S, Caccamo, A, Tran, L, Lambert, MP, Glabe, CG, Klein, WL *et al.* (2006). Temporal profile of amyloid-β (Aβ) oligomerization in an *in vivo* model of Alzheimer disease. A link between Aβ and tau pathology. *J Biol Chem* **281**: 1599–1604.